Advances in Nano Research, *Vol. 10, No. 1 (2021) 1-14*
DOI: https://doi.org/10.12989/anr.2021.10.1.001

Frequency and thermal buckling information of laminated composite doubly curved open nanoshell

Humin Dai*[1] and Hamed Safarpour**[2]

[1]*Department of Advanced Manufacture Technology, Guangdong Mechanical Electrical Polytechnic, Guangzhou, 510515, China*
[2]*Mechanical Engineering department, Faculty of Engineering, Imam Khomeini International University, Qazvin, Iran*

(*Received July 23, 2020, Revised October 12, 2020, Accepted October 15, 2020*)

Abstract. In the present computational approach, thermal buckling and frequency characteristics of a doubly curved laminated nanopanel with the aid of Two-Dimensional Generalized Differential Quadrature Method (2D-GDQM) and Nonlocal Strain Gradient Theory (NSGT) are investigated. Additionally, the temperature changes along the thickness direction nonlinearly. The novelty of the current study is in considering the effects of laminated composite and thermal in addition of size effect on frequency, thermal buckling, and dynamic deflections of the laminated nanopanel. The acquired numerical and analytical results are compared by each other to validate the results. The results demonstrate that some geometrical and physical parameters, have noticeable effects on the frequency and pre-thermal buckling behavior of the doubly curved open cylindrical laminated nanopanel. The favorable suggestion of this survey is that for designing the laminated nano-sized structure should pay special attention to size-dependent parameters because nonlocal and length scale parameters have an important role in the static and dynamic behaviors of the laminated nanopanel.

Keywords: pre-thermal buckling; frequency characteristics; laminated nanopanel; NSGT; nonlinear thermal loading

1. Introduction

Nowadays, due to enhancement in the mechanical behavior (Tounsi *et al*. 2013, Salari 2016, Ebrahimi and Jafari 2017, Ehyaei and Daman 2017, Kumar 2018, Wu *et al*. 2018, Ebrahimi *et al*. 2019a, b, 2020, Ebrahimi and Salari 2019, Emdadi *et al*. 2019, Ghannadpour and Moradi 2019, Hussain *et al*. 2019, Shahsavari *et al*. 2019, Dehshahri *et al*. 2020), acting as a flame retardant, and improving the thermal conductivity, laminated structure has attracted a lot of attention. Thai *et al*. (2019) investigated bending free vibration of buckling characteristics of a laminated plate with the aid of four-variable refined plate theory. In this work, they found that number of laminated layers, and thickness-to-length (h/L) ratio have an important role in the stability of the mentioned structure. Gholami and Ansari (2019) presented the nonlinear frequency analysis of a laminated plate using HSDT. They solved the governing equations with the aid of a multistep numerical solution approach. Free and forced vibration performance of a sandwich plate with viscoelastic core coupled with layers was studied by Ref. (Mohseni and Shakouri 2020). Using Hamilton's principle and classical theory, they developed the governing equations and finally solved them using Navier-type solution procedure. Frequency analysis of a laminated microplate using a size-dependent theory and with the aid of analytical method was introduced by Mohammad-Rezaei Bidgoli and Arefi (2019). One of their golden results was that different parameter of the size-dependent parameter has an essential role in the frequency characteristics of a laminated microplate. The influence of low-velocity impact on the deflection of the laminated plate with geometrical imperfection was presented by Ref. (Song *et al*. 2019). They used Halpin-Tsai and mixture models for calculating the Young's modulus and other material properties, respectively. Resonance characteristics of a laminated plate using Navier solution procedure were studied by Ref. (Karami *et al*. 2019). They modeled the laminated plate via Kirchhoff plate theory and governing equations, and associated boundary conditions were obtained by Hamilton's principle. In this work, they illustrated that the influence of number of layers on the stability of their structure has hardly dependent on the layers. In another work, free vibration analysis of a laminated plate with the aid of a numerical solution procedure was presented by Gunasekaran *et al*. (2020). With the aid of FEM, forced vibration characteristics of a laminated curved plate under high-temperature environment was presented by Ref. (Tran *et al*. 2020). One of the important results that they showed in their work was that geometrical properties of the Graphene Nanoplatelets (GPLs) have an essential influence of the resonance behavior of the laminated curved plate. Recently, the critical temperature of a laminated annular sector plate by considering von Kármán nonlinearity and First-order Shear Deformation Theory (FSDT) was presented by Javani *et al*. (2020). For solving the governing equations, they used

*Corresponding author, Ph.D.,
E-mail: dahumin@163.com
**Co-corresponding author, Professor,
E-mail: hamed.safarpour@edu.ikiu.ac.ir

ISSN: 2287-237X (Print), 2287-2388 (Online)

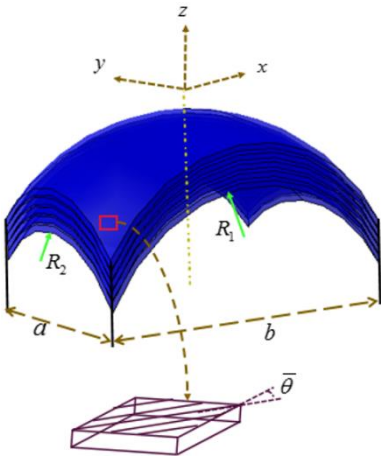

Fig. 1 Schematic of the laminated cylindrical nanopanel subjected to nonlinear thermal loading

GDQM and finally showed that by considering small amount of GPLs into the matrix, critical temperature tends to increases. Due to nanotechnology deployment in various industries, especially in the field of the performance of Micro-Electromechanical System (MEMS), Nano-Electro-Mechanical System (NEMS), and nanostructures, considering the size effect for estimating the thermo-mechanical behaviors of the nanostructure becomes an essential issue (Muc 2011, 2020, Muc and Chwał 2011, Muc and Ulatowska 2012, Arani *et al*. 2019, Arefi *et al*. 2019a, b, 2020a, b, Arefi and Rabczuk 2019, Muc *et al*. 2019, Arefi 2020, Arefi and Civalek 2020, Arefi and Soltan Arani 2020, Żur *et al*. 2020). It has been shown that panels can be used in may industrial and engineering applications (Bai *et al*. 2020). Due to various static and dynamic loads that can fall down the stability of the system, the current structure is often under several environment conditions. Besides, undesirable behaviors may occur for these structures such as buckling, cracks, deformations, and resonance. So, it is very important to know the designer about mechanical behavior of this kind of system to analysis the mentioned structure with the high guarantee reliability. According to the advantage of the GPLs reinforcement, this kind of material can be used as a composite reinforcement in the annular plates. Using 3D-elasticity theory, Yang *et al*. (2017) studied bending analysis of a circular/annular plate. They showed that boundary conditions, distribution patterns, and other geometrically and physically parameters of the GPLs have an essential role in the stress and strain fields of the mentioned structure. The frequency and bending behavior of a laminated annular plate using 3D-elasticity theory were examined by Liu *et al*. (2019). They solved the governing equations of the system with state-space based DQM. They showed that various boundary conditions and other geometrically and physically parameters of structure and GPLs play important role in the frequency and bending characteristics of the laminated annular plate. Wang *et al*. (2020) investigated frequency analysis of a thermally affected laminated annular plate using GDQM. They showed that various thermal distribution and locating more square-shaped GPLs can be improved the dynamic behavior of the laminated annular plate in thermal environment. Nonlinear forced vibration analysis of the laminated annular plate in a high-temperature environment was introduced by Wu *et al*. (2020). Using GDQM and iterative method, they solved the nonlinear governing equations and boundary conditions. Finally, they illustrated that the nonlinear frequency ratio decreases when they put more GPLs within the outer layers of the laminated annular plate. Rotating plates and disks and have a lot of applications such as, computer disks, compressors, rotors, and pump. For this issue, in the field of stability/instability analysis of the rotating annular/circular plate, Hu and Wang (2016) investigated nonlinear behavior of the rotating circular plate under magnetic excitation. Their presented structure was modeled via thin plate theory, and finally, they solved the nonlinear governing equations via Galerkin and multiple scales methods. They showed that, angular velocity and magnetic field have an essential role in the stability/ instability of the rotating circular plate. Stability analysis of an isotropic homogeneous spinning annular plate was presented by Ref. (Bagheri *et al*. 2019). With the aid of FSDT and von Kármán nonlinearity the model had been extracted. Mahinzare *et al*. (2018) examined frequency behavior of a smart rotating Functionally Graded (FG) circular plate with the aid of classical theory. They solved the governing equations using DQM. They illustrated that associated parameters to FG, external voltage and angular speed of rotation have essential role in the frequency characteristics of the smart (FG) circular plate. In another work, Qin *et al*. (2018) investigated vibrational charactrestics of the cylindrical shell coupled with annular disk in the framework of analytical based Rayleigh-Ritz method. Recently, influence of hygro-thermal environment of the multi-field responses of the imperfect Magneto-Electro-Elastic (MEE) annular plate was presented by Ref. (Dai *et al*. 2019). Via steady-state heat conduction the thermal environment had been modeled. Finally, using DQM the governing equation were solved and the results showed the influence of the external conditions (moisture and temperature) on the multi-field responses of the imperfect MEE annular plate.

Also, Refs. (Tornabene 2009, Tornabene and Viola 2009, Tornabene *et al*. 2009, 2013, 2014, 2015a, b, 2016, 2017, Viola and Tornabene 2009, Nguyen-Thanh *et al*. 2010, Natarajan *et al*. 2012, Thai *et al*. 2012, Nguyen-Thoi *et al*. 2013, 2014, 2017, Valizadeh *et al*. 2013, Viola *et al*. 2013, Sahmani *et al*. 2018, Khosravi *et al*. 2020, Noroozi *et al*. 2020, Sofiyev *et al*. 2020) presented stability/instability analysis of the structures with the aid of different solution procedure.

For the first time, the presented study investigates the thermal buckling and frequency analysis of a laminated nanopanel taking into consideration NSGT and exact values of nonlocalities and length scale parameters. The dynamic equations of the composite nanostructure are based on FSDT and 2D-GDQM is implemented to solve these equations and obtain the natural frequency of the current model. Eventually, the current study has been made into the influences of R_1/a, NSG parameters and geometric

parameters on the dynamic and static stability of the laminated nanostructure employing the continuum mechanics model.

2. Theory and formualtion

A laminated nanopanel in the thermal environment is seen in Fig. 1

2.1 Displacement fields

On the basis of Higher-Order Shear Deformation Theory (HOSDT), The displacement field can be stated as (Karimiasl *et al*. 2019).

$$\begin{aligned}(x,y,z,t) &= u_0(x,y,t) + z\phi_x(x,y,t) \\ &\quad - c_1 z^3 \times \left[\frac{\partial w_0(x,y,t)}{\partial x} + \phi_x(x,y,t)\right] \\ v(x,y,z,t) &= v_0(x,y,t) + z\phi_y(x,y,t) \\ &\quad - c_1 z^3 \times \left[\frac{\partial w_0(x,y,t)}{\partial y} + \phi_y(x,y,t)\right] \\ w(x,y,z,t) &= w_0(x,y,t)\end{aligned} \tag{1}$$

The strain components can be given by

$$\begin{Bmatrix}\varepsilon_{xx}\\ \varepsilon_{yy}\\ \gamma_{xy}\\ \gamma_{xz}\\ \gamma_{yz}\end{Bmatrix} = \begin{bmatrix}\frac{\partial u_0}{\partial x} + z\frac{\partial \phi_x}{\partial x} - z^3 c_1\left(\frac{\partial \phi_x}{\partial x} + \frac{\partial^2 w_0}{\partial x^2}\right)\\ \frac{\partial v_0}{\partial y} + z\frac{\partial \phi_x}{\partial y} - z^3 c_1\left(\frac{\partial \phi_y}{\partial y} + \frac{\partial^2 w_0}{\partial y^2}\right)\\ \frac{\partial u_0}{\partial y} + \frac{\partial v_0}{\partial x} + z\left(\frac{\partial \phi_x}{\partial y} + \frac{\partial \phi_y}{\partial x}\right) - z^3 c_1\left(\frac{\partial \phi_x}{\partial y} + \frac{\partial \phi_y}{\partial x} + 2\frac{\partial^2 w_0}{\partial x \partial y}\right)\\ (1-3z^2c_1)\left(\phi_x + \frac{\partial w_0}{\partial x}\right)\\ (1-3z^2c_1)\left(\phi_y + \frac{\partial w_0}{\partial y}\right)\end{bmatrix} \tag{2}$$

where c_1 is expressed as $4/3h^2$ in HOSDT. The stress-strain relation can be expressed as follows

$$\begin{aligned}(1-\mu^2\nabla^2)\begin{bmatrix}t_{xx}\\ t_{\theta\theta}\\ t_{x\theta}\end{bmatrix} &= (1-l^2\nabla^2)\begin{bmatrix}C_{11} & C_{12} & 0\\ C_{12} & C_{22} & 0\\ 0 & 0 & C_{66}\end{bmatrix}^{(L)}\begin{bmatrix}\varepsilon_{xx}\\ \varepsilon_{\theta\theta}\\ \varepsilon_{x\theta}\end{bmatrix} \\ (1-\mu^2\nabla^2)\begin{bmatrix}t_{\theta z}\\ t_{xz}\end{bmatrix} &= (1-l^2\nabla^2)\begin{bmatrix}C_{44} & 0\\ 0 & C_{55}\end{bmatrix}^{(L)}\begin{bmatrix}\varepsilon_{\theta z}\\ \varepsilon_{xz}\end{bmatrix}\end{aligned} \tag{3}$$

in which the coefficients of the C_{ij} matrix, known as the reduced elastic constants of the orthotropic material corresponding to L^{th} lamina, are expressed as follows

$$\begin{aligned}C_{11} &= Q_{11}\,\bar{cos}^4\theta + 2(Q_{12}+2Q_{44})\,\bar{sin}^2\theta\,\bar{cos}^2\theta \\ &\quad + Q_{22}\,\bar{sin}^4\theta \\ C_{12} &= (Q_{11}+Q_{22}-4Q_{44})\,\bar{sin}^2\theta\,\bar{cos}^2\theta \\ &\quad + Q_{12}(\bar{sin}^4\theta + \bar{cos}^4\theta) \\ C_{22} &= Q_{11}\,\bar{sin}^4\theta + 2(Q_{12}+2Q_{44})\,\bar{sin}^2\theta\,\bar{cos}^2\theta \\ &\quad + Q_{22}\,\bar{cos}^4\theta \\ C_{44} &= Q_{44}\,\bar{cos}^4\theta + Q_{55}\,\bar{sin}^4\theta \\ C_{55} &= Q_{55}\,\bar{cos}^4\theta + Q_{66}\,\bar{sin}^4\theta \\ C_{66} &= (Q_{11}+Q_{22}-2Q_{12})\,\bar{sin}^2\theta\,\bar{cos}^2\theta \\ &\quad + Q_{66}(\bar{cos}^2\theta - \bar{sin}^2\theta)^2\end{aligned} \tag{4}$$

As mentioned earlier, the relations given by Eq. (5) are stress-strain constitutive relations for the *L*th orthotropic lamina referred to as the lamina's principal material axes x, θ and z. In Eq. (4), $\bar{\theta}$ is fiber angle and Q_{ij} is defined as follows (Karimiasl *et al*. 2019)

$$\begin{aligned}Q_{11} &= \frac{E_1}{1-\nu_{12}\nu_{21}}, \qquad Q_{12} = \frac{\nu_{12}E_2}{1-\nu_{12}\nu_{21}} \\ Q_{22} &= \frac{E_2}{1-\nu_{12}\nu_{21}} \\ Q_{66} &= G_{12}, \qquad Q_{44} = G_{23}, \qquad Q_{55} = G_{13}\end{aligned} \tag{5}$$

2.2 Extended Hamilton's principle

By using Hamilton's principle and fundamental Lemma of the calculus of variations, the governing equations and their related boundary conditions are acquired as (Karimiasl *et al*. 2019)

$$\int_{t_1}^{t_2}(\delta W + \delta T - \delta U)dt = 0 \tag{6}$$

The parameters of T and U are the kinetic and strain energy, respectively.

$$\begin{aligned}&T = \int_V 0.5\times\rho\left[\left(\frac{\partial u}{\partial t}\right)^2 + \left(\frac{\partial v}{\partial t}\right)^2 + \left(\frac{\partial w}{\partial t}\right)^2\right]dV: \\ &\delta T = \\ &\int_0^a\int_0^b\left[\left(-I_0\frac{\partial^2 u_0}{\partial t^2} - I_1\frac{\partial^2\phi_x}{\partial t^2} + I_3c_1\left(\frac{\partial^2\phi_x}{\partial t^2} + \frac{\partial^3 w_0}{\partial t^2\partial x}\right)\right)\delta u_0\right. \\ &+\left(-I_1\frac{\partial^2 u_0}{\partial t^2} - I_2\frac{\partial^2\phi_x}{\partial t^2} + I_4c_1\left(\frac{\partial^2\phi_x}{\partial t^2} + \frac{\partial^3 w}{\partial t^2\partial x}\right)\right)\delta\phi_x \\ &+\left(c_1I_3\frac{\partial^2 u_0}{\partial t^2} + c_1I_4\frac{\partial^2\phi_x}{\partial t^2} - I_6{c_1}^2\left(\frac{\partial^2\phi_x}{\partial t^2} + \frac{\partial^3 w}{\partial t^2\partial x}\right)\right)\delta\phi_x \\ &+\left(-c_1I_3\frac{\partial^3 u_0}{\partial x\partial t^2} - c_1I_4\frac{\partial^3\phi_x}{\partial x\partial t^2} + I_6{c_1}^2\left(\frac{\partial^3\phi_x}{\partial x\partial t^2} + \frac{\partial^4 w}{\partial t^2\partial x^2}\right)\right) \\ &\delta w_0\left(-I_0\frac{\partial^2 v_0}{\partial t^2} - I_1\frac{\partial^2\phi_y}{\partial t^2} + I_3c_1\left(\frac{\partial^2\phi_y}{\partial t^2} + \frac{\partial^3 w_0}{\partial t^2\partial y}\right)\right)\delta v_0 \\ &+\left(-I_1\frac{\partial^2 v_0}{\partial t^2} - I_2\frac{\partial^2\phi_y}{\partial t^2} + I_4c_1\left(\frac{\partial^2\phi_y}{\partial t^2} + \frac{\partial^3 w}{\partial t^2\partial y}\right)\right)\delta\phi_y \\ &+\left(c_1I_3\frac{\partial^2 v_0}{\partial t^2} + c_1I_4\frac{\partial^2\phi_y}{\partial t^2} - I_6{c_1}^2\left(\frac{\partial^2\phi_y}{\partial t^2} + \frac{\partial^3 w}{\partial t^2\partial y}\right)\right)\delta\phi_y \\ &+\left(-c_1I_3\frac{\partial^3 v_0}{\partial y\partial t^2} - c_1I_4\frac{\partial^3\phi_y}{\partial y\partial t^2} + I_6{c_1}^2\left(\frac{\partial^3\phi_y}{\partial y\partial t^2} + \frac{\partial^4 w}{\partial t^2\partial y^2}\right)\right) \\ &\left.\delta w_0 + \left(-I_0\frac{\partial^2 w_0}{\partial t^2}\right)\delta w_0\right.\end{aligned} \tag{7}$$

in which

$$\begin{aligned}&\{I_0, I_1, I_2, I_3, I_4, I_5, I_6\} \\ &= \int_{-h/2}^{h/2}\rho\{1, z, z^2, z^3, z^4, z^5, z^6\}(1+\frac{z}{R_1})(1+\frac{z}{R_2})dz\end{aligned} \tag{8}$$

and

$$\delta U = \frac{1}{2}\iiint_V \sigma_{ij}\delta\varepsilon_{ij}dV = \iint_A \begin{bmatrix} N_{xx}\frac{\partial\delta u_0}{\partial x} + M_{xx}\frac{\partial\delta\phi_x}{\partial x} - P_{xx}c_1\left(\frac{\partial\delta\phi_x}{\partial x} + \frac{\partial^2\delta w_0}{\partial x^2}\right) \\ +N_{yy}\frac{\partial\delta v_0}{\partial y} + M_{yy}\frac{\partial\delta\phi_x}{\partial y} - P_{yy}c_1\left(\frac{\partial\delta\phi_y}{\partial y} + \frac{\partial^2\delta w_0}{\partial y^2}\right) \\ +N_{xy}\frac{\partial\delta u_0}{\partial y} + N_{xy}\frac{\partial\delta v_0}{\partial x} + M_{xy}\left(\frac{\partial\delta\phi_x}{\partial y} + \frac{\partial\delta\phi_y}{\partial x}\right) \\ -P_{xy}c_1\left(\frac{\partial\delta\phi_x}{\partial y} + \frac{\partial\delta\phi_y}{\partial x} + 2\frac{\partial^2\delta w_0}{\partial x\partial y}\right) \\ +(Q_{xz} - 3S_{xz}c_1)\left(\delta\phi_x + \frac{\partial\delta w_0}{\partial x}\right) + (Q_{yz} - 3S_{yz}c_1)\left(\delta\phi_y + \frac{\partial\delta w_0}{\partial y}\right) \end{bmatrix} dA =$$

$$\iint_A \begin{bmatrix} -\left(\frac{\partial}{\partial x}N_{xx}\right)\delta u_0 - \left(\frac{\partial}{\partial x}M_{xx}\right)\delta\phi_x + c_1 \times \begin{pmatrix} \left(\frac{\partial}{\partial x}P_{xx}\right)\delta\phi_x \\ -\left(\frac{\partial^2}{\partial x^2}P_{xx}\right)\delta w_0 \end{pmatrix} \\ -\left(\frac{\partial}{\partial y}N_{yy}\right)\delta v_0 - \left(\frac{\partial}{\partial y}M_{yy}\right)\delta\phi_y + c_1 \times \begin{pmatrix} \left(\frac{\partial}{\partial y}P_{yy}\right)\delta\phi_y \\ -\left(\frac{\partial^2}{\partial y^2}P_{yy}\right)\delta w_0 \end{pmatrix} \\ -\left(\frac{\partial}{\partial y}N_{xy}\right)\delta u_0 - \left(\frac{\partial}{\partial x}N_{xy}\right)\delta v_0 - \left(\frac{\partial}{\partial y}M_{xy}\right)\delta\phi_x - \left(\frac{\partial}{\partial x}M_{xy}\right)\delta\phi_y \\ +c_1 \times \left(\left(\frac{\partial}{\partial y}P_{xy}\right)\delta\phi_x + \left(\frac{\partial}{\partial x}P_{xy}\right)\delta\phi_y - 2 \times \left(\frac{\partial^2}{\partial x\partial y}P_{xy}\right)\delta w_0\right) \\ +(Q_{xz})\delta\phi_x - \left(\frac{\partial}{\partial x}Q_{xz}\right)\delta w_0 - 3 \times c_1 \times \left((S_{xz})\delta\phi_x - \left(\frac{\partial}{\partial x}S_{xz}\right)\delta w_0\right) \\ +(Q_{yz})\delta\phi_y - \left(\frac{\partial}{\partial y}Q_{yz}\right)\delta w_0 - 3 \times c_1 \times \left((S_{yz})\delta\phi_y - \left(\frac{\partial}{\partial y}S_{yz}\right)\delta w_0\right) \end{bmatrix} dA \tag{9}$$

which

$$\{N_{xy}, N_{yy}, N_{xx}\} = \int_z \{\sigma_{xy}, \sigma_{yy}, \sigma_{xx}\}\, dz, \qquad \{M_{xy}, M_{yy}, M_{xx}\} = \int_z \{\sigma_{xy}, \sigma_{yy}, \sigma_{xx}\} \times z dz$$
$$\{P_{xy}, P_{yy}, P_{xx}\} = \int_z \{\sigma_{xy}, \sigma_{yy}, \sigma_{xx}\} \times z^3 dz, \qquad \{Q_{yz}, Q_{xz}\} = \int_z \{\sigma_{xy}, \sigma_{xz}\}\, dz, \qquad \{S_{yz}, S_{xz}\} = \int_z \{\sigma_{xy}, \sigma_{xz}\} \times z^2\, dz \tag{10}$$

So

$$\begin{aligned}
N_{xx} &= A_{11}\frac{\partial u_0}{\partial x} + B_{11}\frac{\partial\phi_x}{\partial x} - D_{11}c_1\left(\frac{\partial\phi_x}{\partial x} + \frac{\partial^2 w_0}{\partial x^2}\right) + A_{12}\frac{\partial v_0}{\partial y} + B_{12}\frac{\partial\phi_y}{\partial y} - D_{12}c_1\left(\frac{\partial\phi_y}{\partial y} + \frac{\partial^2 w_0}{\partial y^2}\right) \\
N_{yy} &= A_{22}\frac{\partial v_0}{\partial y} + B_{22}\frac{\partial\phi_y}{\partial y} - D_{22}c_1\left(\frac{\partial\phi_y}{\partial y} + \frac{\partial^2 w_0}{\partial y^2}\right) + A_{12}\frac{\partial u_0}{\partial x} + B_{12}\frac{\partial\phi_x}{\partial x} - D_{12}c_1\left(\frac{\partial\phi_x}{\partial x} + \frac{\partial^2 w_0}{\partial x^2}\right) \\
N_{xy} &= A_{44}\frac{\partial u_0}{\partial y} + A_{44}\frac{\partial v_0}{\partial x} + B_{44}\left(\frac{\partial\phi_x}{\partial y} + \frac{\partial\phi_y}{\partial x}\right) - D_{44}c_1\left(\frac{\partial\phi_x}{\partial y} + \frac{\partial\phi_y}{\partial x} + 2\frac{\partial^2 w_0}{\partial x\partial y}\right) \\
M_{xx} &= B_{11}\frac{\partial u_0}{\partial x} + C_{11}\frac{\partial\phi_x}{\partial x} - E_{11}c_1\left(\frac{\partial\phi_x}{\partial x} + \frac{\partial^2 w_0}{\partial x^2}\right) + B_{12}\frac{\partial v_0}{\partial y} + C_{12}\frac{\partial\phi_y}{\partial y} - E_{12}c_1\left(\frac{\partial\phi_y}{\partial y} + \frac{\partial^2 w_0}{\partial y^2}\right) \\
M_{yy} &= B_{22}\frac{\partial v_0}{\partial y} + C_{22}\frac{\partial\phi_y}{\partial y} - E_{22}c_1\left(\frac{\partial\phi_y}{\partial y} + \frac{\partial^2 w_0}{\partial y^2}\right) + B_{12}\frac{\partial u_0}{\partial x} + C_{12}\frac{\partial\phi_x}{\partial x} - E_{12}c_1\left(\frac{\partial\phi_x}{\partial x} + \frac{\partial^2 w_0}{\partial x^2}\right) \\
M_{xy} &= B_{44}\frac{\partial u_0}{\partial y} + B_{44}\frac{\partial v_0}{\partial x} + C_{44}\left(\frac{\partial\phi_x}{\partial y} + \frac{\partial\phi_y}{\partial x}\right) - E_{44}c_1\left(\frac{\partial\phi_x}{\partial y} + \frac{\partial\phi_y}{\partial x} + 2\frac{\partial^2 w_0}{\partial x\partial y}\right) \\
p_{xx} &= D_{11}\frac{\partial u_0}{\partial x} + E_{11}\frac{\partial\phi_x}{\partial x} - G_{11}c_1\left(\frac{\partial\phi_x}{\partial x} + \frac{\partial^2 w_0}{\partial x^2}\right) + D_{12}\frac{\partial v_0}{\partial y} + E_{12}\frac{\partial\phi_y}{\partial y} - G_{12}c_1\left(\frac{\partial\phi_y}{\partial y} + \frac{\partial^2 w_0}{\partial y^2}\right) \\
p_{yy} &= D_{22}\frac{\partial v_0}{\partial y} + E_{22}\frac{\partial\phi_y}{\partial y} - G_{22}c_1\left(\frac{\partial\phi_y}{\partial y} + \frac{\partial^2 w_0}{\partial y^2}\right) + D_{12}\frac{\partial u_0}{\partial x} + E_{12}\frac{\partial\phi_x}{\partial x} - G_{12}c_1\left(\frac{\partial\phi_x}{\partial x} + \frac{\partial^2 w_0}{\partial x^2}\right) \\
p_{xy} &= D_{44}\frac{\partial u_0}{\partial y} + D_{44}\frac{\partial v_0}{\partial x} + E_{44}\left(\frac{\partial\phi_x}{\partial y} + \frac{\partial\phi_y}{\partial x}\right) - G_{44}c_1\left(\frac{\partial\phi_x}{\partial y} + \frac{\partial\phi_y}{\partial x} + 2\frac{\partial^2 w_0}{\partial x\partial y}\right), \qquad Q_{xz} = (A_{55} - 3C_{55}c_1)\left(\phi_x + \frac{\partial w_0}{\partial x}\right) \\
S_{xz} &= (C_{55} - 3E_{55}c_1)\left(\phi_x + \frac{\partial w_0}{\partial x}\right), \qquad Q_{yz} = (A_{66} - 3C_{66}c_1)\left(\phi_y + \frac{\partial w_0}{\partial y}\right), \qquad S_{yz} = (C_{66} - 3E_{66}c_1)\left(\phi_y + \frac{\partial w_0}{\partial y}\right)
\end{aligned} \tag{11}$$

and

$$\begin{aligned}
&\{A_{11},B_{11},C_{11},D_{11},E_{11},F_{11},G_{11}\}=\\
&\int_{-\frac{h}{2}}^{\frac{h}{2}}Q_{11}\times\{1,z,z^2,z^3,z^4,z^5,z^6\}\times\left(1+\frac{z}{R_1}\right)\times\left(1+\frac{z}{R_2}\right)dz\\
&\{A_{12},B_{12},C_{12},D_{12},E_{12},F_{12},G_{12}\}=\\
&\int_{-\frac{h}{2}}^{\frac{h}{2}}Q_{12}\times\{1,z,z^2,z^3,z^4,z^5,z^6\}\times\left(1+\frac{z}{R_1}\right)\times\left(1+\frac{z}{R_2}\right)dz\\
&\{A_{22},B_{22},C_{22},D_{22},E_{22},F_{22},G_{22}\}=\\
&\int_{-\frac{h}{2}}^{\frac{h}{2}}Q_{22}\times\{1,z,z^2,z^3,z^4,z^5,z^6\}\times\left(1+\frac{z}{R_1}\right)\times\left(1+\frac{z}{R_2}\right)dz\\
&\{A_{44},B_{44},C_{44},D_{44},E_{44}\}=\\
&\int_{-\frac{h}{2}}^{\frac{h}{2}}Q_{44}\times\{1,z,z^2,z^3,z^4\}\times\left(1+\frac{z}{R_1}\right)\times\left(1+\frac{z}{R_2}\right)dz\\
&\{A_{55},B_{55},C_{55},D_{55},E_{55}\}=\\
&\int_{-\frac{h}{2}}^{\frac{h}{2}}Q_{55}\times\{1,z,z^2,z^3,z^4\}\times\left(1+\frac{z}{R_1}\right)\times\left(1+\frac{z}{R_2}\right)dz\\
&\{A_{66},B_{66},C_{66},D_{66},E_{66}\}\\
&=\int_{-h/2}^{h/2}Q_{66}\times\{1,z,z^2,z^3,z^4\}\times(1+z/R_1)\times(1+z/R_2)dz
\end{aligned}\tag{12}$$

2.3 Nonlinear temperature changes

The parameter of W is the work done by temperature changes and is declared as following (SafarPour *et al*. 2017)

$$W=\frac{1}{2}\iint_A\left[(N_2^C)(\frac{\partial w_0}{\partial x})^2+(N_1^C)(\frac{\partial v_0}{\partial x})^2\right](1+\frac{z}{R_1})(1+\frac{z}{R_2})dxdy\tag{13}$$

where the thermal stress resultants are defined with the following relations

$$\begin{aligned}
N_1^C&=\int_{-h/2}^{h/2}(T-T_0)\times\alpha\times(\bar{Q}_{12}+\bar{Q}_{11})dz\\
N_2^C&=\int_{-h/2}^{h/2}(T-T_0)\times\alpha\times(\bar{Q}_{22}+\bar{Q}_{21})dz\\
T&=T_c-\sum_{n=1}^{\infty}(T_c-T_m)\times(z/h+1/2)^n
\end{aligned}\tag{14}$$

where n denotes the non-negative power index of temperature variation function. For example, considering $n \geq 2$ the temperature variation along the thickness becomes nonlinear (Shafiei *et al*. 2017). The thermal expansion coefficients are

$$\alpha=[\alpha_1\alpha_2000]^T\tag{15}$$

It is assumed that the temperature changes nonlinearly through the thickness direction from the external surface (T_m) to the internal surface (T_c). Eventually, the motion equations are achieved as follows

$$\begin{aligned}
&u_0\colon \frac{\partial N_{xx}}{\partial x}+\frac{\partial N_{xy}}{\partial y}\\
&=I_0\frac{\partial^2u_0}{\partial t^2}+I_1\frac{\partial^2\phi_x}{\partial t^2}-I_3c_1\left(\frac{\partial^2\phi_x}{\partial t^2}+\frac{\partial^3w_0}{\partial t^2\partial x}\right)\\
&\delta v_0\colon \frac{\partial N_{yy}}{\partial y}+\frac{\partial N_{xy}}{\partial x}-N_1^c\frac{\partial^2v_0}{\partial x^2}\\
&=I_0\frac{\partial^2v_0}{\partial t^2}+I_1\frac{\partial^2\phi_y}{\partial t^2}-I_3c_1\left(\frac{\partial^2\phi_y}{\partial t^2}+\frac{\partial^3w_0}{\partial t^2\partial y}\right)\\
&\delta w_0\colon\ c_1\frac{\partial^2P_{xx}}{\partial x^2}+c_1\frac{\partial^2P_{yy}}{\partial y^2}+2c_1\frac{\partial^2P_{xy}}{\partial x\partial y}+\frac{\partial Q_{xz}}{\partial x}\\
&-3c_1\frac{\partial S_{xz}}{\partial x}+\frac{\partial Q_{yz}}{\partial y}-3c_1\frac{\partial S_{yz}}{\partial y}-\left[\frac{N_{xx}}{R_1}+\left(\frac{\partial^2N_{xx}}{\partial x^2}\right)\right]\\
&-\left[\frac{N_{yy}}{R_2}+\left(\frac{\partial^2N_{yy}}{\partial y^2}\right)\right]+2\frac{\partial^2N_{xy}}{\partial x\partial y}-N_2^c\frac{\partial^2w_0}{\partial x^2}=\\
&c_1I_3\frac{\partial^3u_0}{\partial x\partial t^2}+c_1I_4\frac{\partial^3\phi_x}{\partial x\partial t^2}-I_6{c_1}^2\left(\frac{\partial^3\phi_x}{\partial x\partial t^2}+\frac{\partial^4w}{\partial t^2\partial x^2}\right)\\
&+c_1I_3\frac{\partial^3v_0}{\partial y\partial t^2}+c_1I_4\frac{\partial^3\phi_y}{\partial y\partial t^2}-I_6{c_1}^2\left(\frac{\partial^3\phi_y}{\partial y\partial t^2}+\right.\\
&\left.\frac{\partial^4w}{\partial t^2\partial y^2}\right)+\left(I_0\frac{\partial^2w_0}{\partial t^2}\right)
\end{aligned}\tag{16}$$

And the corresponding boundary conditions are defined as

$$\begin{aligned}
&\text{Simply at}\ \ x=0,\quad a\to M_{xx}-c_1P_{xx}=0,\\
&N_{xx}=0,\quad \phi_y=0,\quad W=0,\quad V=0\\
&\text{Simply at}\ \ y=0,\quad b\to M_{yy}-c_1P_{yy}=0,\\
&N_{yy}=0,\quad \phi_x=0,\quad W=0,\quad U=0\\
&\text{Clamped at}\ \ x=0,\quad a\to\phi_y=0,\quad \phi_x=0,\\
&U=0,\quad W=0,\quad V=0\\
&\text{Clamped at}\ \ x=0,\quad a\to\phi_y=0,\quad \phi_x=0,\\
&U=0,\quad W=0,\quad V=0\\
&\text{Free at}\ \ x=0,\quad a\to N_{xx}=0,\\
&M_{xx}-c_1P_{xx}=0,\quad N_{xy}=0,\quad M_{xy}-c_1P_{xy}=0,\\
&-c_1P_{xx}+c_1\frac{\partial P_{xx}}{\partial x}-2c_1\frac{\partial P_{xy}}{\partial y}+(Q_{xz}-3c_1S_{xz}),\\
&\text{Free at}\ \ y=0,\quad b\to N_{yy}=0,\\
&M_{yy}-c_1P_{yy}=0,\quad N_{xy}=0,\quad M_{xy}-c_1P_{xy}=0,\\
&-c_1P_{yy}+c_1\frac{\partial P_{yy}}{\partial y}-2c_1\frac{\partial P_{xy}}{\partial x}+(Q_{yz}-3c_1S_{yz})
\end{aligned}\tag{17}$$

2.4 NSGT for size-dependent nanostructure

In the present work, by considering the NSG theory, the influences of size-dependent are investigated in the mathematical model. On the basis of this theory, stress-strain relations are presented as (Malikan *et al*. 2018, Mahinzare *et al*. 2019)

$$\begin{aligned}
&(1-\mu^2\nabla^2)\times t_{ij}\\
&=C_{ijck}\times(1-l^2\nabla^2)\times\varepsilon_{ck}
\end{aligned}\tag{18}$$

where $\nabla^2=\partial^2/\partial x^2+\partial^2/\partial y^2$; C_{ijck} , ε_{ck} and t_{ij} represent the components of NSG elasticity, strain and stress tensors, respectively. The generalized relationship between strain and stress can be demonstrated as

$$(1-\mu^2\nabla^2)t_{ij}=(1-l^2\nabla^2)Q_{ij}\varepsilon_{ij}\tag{19}$$

Eventually, motion equations of the thermally affected nano panel utilizing NSG theory are acquired as follows

$$
\begin{aligned}
&\delta u_0\colon (1-\nabla^2 l^2)\left(\frac{\partial N_{xx}}{\partial x}+\frac{\partial N_{xy}}{\partial y}\right)=(1-\nabla^2\mu^2)\left(I_0\frac{\partial^2 u_0}{\partial t^2}+I_1\frac{\partial^2\phi_x}{\partial t^2}-I_3c_1\left(\frac{\partial^2\phi_x}{\partial t^2}+\frac{\partial^3 w_0}{\partial t^2\partial x}\right)\right)\\
&\delta v_0\colon (1-\nabla^2 l^2)\left(\frac{\partial N_{yy}}{\partial y}+\frac{\partial N_{xy}}{\partial x}-N_1^C(\frac{\partial^2 v_0}{\partial x^2})\right)=(1-\nabla^2\mu^2)\left(I_0\frac{\partial^2 v_0}{\partial t^2}+I_1\frac{\partial^2\phi_y}{\partial t^2}-I_3c_1\left(\frac{\partial^2\phi_y}{\partial t^2}+\frac{\partial^3 w_0}{\partial t^2\partial y}\right)\right)\\
&\delta w_0\colon (1-\nabla^2 l^2)\begin{pmatrix}c_1\frac{\partial^2 P_{xx}}{\partial x^2}+c_1\frac{\partial^2 P_{yy}}{\partial y^2}+2c_1\frac{\partial^2 P_{xy}}{\partial x\partial y}+\frac{\partial Q_{xz}}{\partial x}\\-3c_1\frac{\partial S_{xz}}{\partial x}+\frac{\partial Q_{yz}}{\partial y}-3c_1\frac{\partial S_{yz}}{\partial y}+2\frac{\partial^2 N_{xy}}{\partial x\partial y}-N_2^C(\frac{\partial^2 w_0}{\partial x^2})\\-\left[\frac{N_{xx}}{R_1}+(\frac{\partial^2 N_{xx}}{\partial x^2})\right]-\left[\frac{N_{yy}}{R_2}+(\frac{\partial^2 N_{yy}}{\partial y^2})\right]\end{pmatrix}=\\
&(1-\nabla^2\mu^2)\begin{pmatrix}c_1I_3\frac{\partial^3 u_0}{\partial x\partial t^2}+c_1I_4\frac{\partial^3\phi_x}{\partial x\partial t^2}-I_6{c_1}^2\left(\frac{\partial^3\phi_x}{\partial x\partial t^2}+\frac{\partial^4 w}{\partial t^2\partial x^2}\right)+c_1I_3\frac{\partial^3 v_0}{\partial y\partial t^2}\\-I_6{c_1}^2\left(\frac{\partial^3\phi_y}{\partial y\partial t^2}+\frac{\partial^4 w}{\partial t^2\partial y^2}\right)+\left(I_0\frac{\partial^2 w_0}{\partial t^2}\right)+c_1I_4\frac{\partial^3\phi_y}{\partial y\partial t^2}\end{pmatrix}\\
&\delta\phi_x\colon (1-\nabla^2 l^2)\left(\frac{\partial M_{xx}}{\partial x}-c_1\frac{\partial P_{xx}}{\partial x}+\frac{\partial M_{xy}}{\partial y}-c_1\frac{\partial P_{xy}}{\partial y}-Q_{xz}+3c_1S_{xz}\right)=\\
&(1-\nabla^2\mu^2)\begin{pmatrix}I_1\frac{\partial^2 u_0}{\partial t^2}+I_2\frac{\partial^2\phi_x}{\partial t^2}-I_4c_1\left(\frac{\partial^2\phi_x}{\partial t^2}+\frac{\partial^3 w}{\partial t^2\partial x}\right)-c_1I_3\frac{\partial^2 u_0}{\partial t^2}-c_1I_4\frac{\partial^2\phi_x}{\partial t^2}\\+I_6{c_1}^2\left(\frac{\partial^2\phi_x}{\partial t^2}+\frac{\partial^3 w}{\partial t^2\partial x}\right)\end{pmatrix}\\
&\delta\phi_y\colon (1-\nabla^2 l^2)\left(\frac{\partial M_{yy}}{\partial y}-c_1\frac{\partial P_{yy}}{\partial y}+\frac{\partial M_{xy}}{\partial x}-c_1\frac{\partial P_{xy}}{\partial x}-Q_{yz}+3c_1S_{yz}\right)=\\
&(1-\nabla^2\mu^2)\begin{pmatrix}I_1\frac{\partial^2 v_0}{\partial t^2}+I_2\frac{\partial^2\phi_y}{\partial t^2}-I_4c_1\left(\frac{\partial^2\phi_y}{\partial t^2}+\frac{\partial^3 w}{\partial t^2\partial y}\right)-c_1I_3\frac{\partial^2 v_0}{\partial t^2}\\-c_1I_4\frac{\partial^2\phi_y}{\partial t^2}+I_6{c_1}^2\left(\frac{\partial^2\phi_y}{\partial t^2}+\frac{\partial^3 w}{\partial t^2\partial y}\right)\end{pmatrix}
\end{aligned}
\tag{20}
$$

It is worth mentioning that, $\nabla^2=\partial^2/\partial x^2+\partial^2/\partial y^2$.

3. Solution procedure

3.1 Analytical method

Fourier series expansion for displacement components according to the following relations satisfies simply supported boundary conditions (Karimiasl *et al*. 2019)

$$
\begin{Bmatrix}u(x,y,z)\\v(x,y,z)\\w(x,y,z)\\\phi_x(x,y,z)\\\phi_y(x,y,z)\end{Bmatrix}=\sum_{m=1}^{\infty}\sum_{n=1}^{\infty}\begin{Bmatrix}U_{mn}\times cos\frac{m\pi x}{a}\times sin\frac{n\pi y}{b}\times e^{\omega t}\\V_{mn}\times sin\frac{m\pi x}{a}\times cos\frac{n\pi y}{b}\times e^{\omega t}\\W_{mn}\times sin\frac{m\pi x}{a}\times sin\frac{n\pi y}{b}\times e^{\omega t}\\\Phi_{mnx}\times cos\frac{m\pi x}{a}\times sin\frac{n\pi y}{b}\times e^{\omega t}\\\Phi_{mny}\times sin\frac{m\pi x}{a}\times cos\frac{n\pi y}{b}\times e^{\omega t}\end{Bmatrix}
\tag{21}
$$

Substitution of Eq. (22) into the governing equations, the natural frequency would be attained as follows

$$
K-M\omega^2=0
\tag{22}
$$

where K, M and ω represent the stiffness, mass matrixes and natural frequency, respectively.

3.2 Numerical method

In this section, for other edges of boundary conditions, it is not possible to solve the equation of motion analytically. In this paper, GDQM is utilized to solve the governing equations. The nth derivative of any arbitrary function as $f_{(x,y)}$ can be written in the summation form as follow

$$
\frac{\partial^n f}{\partial R^n}=\sum_{m=1}^{M}C^{(n)}{}_{j,m}f_{m,k}
\tag{23}
$$

which $C^{(n)}$ represent the n^{th}-order derivative of weighting coefficients. And, the calculation of the $C^{(n)}$ is an important part of the DQ method. To estimate the n^{th} order radial derivatives, two types of DQ method combined of the GDQ method are adopted in the present work. Consequently, by utilizing the first-order derivative, $C^{(n)}$ is calculated as follows

$$
\begin{aligned}
&C_{ij}^{(1)}=\frac{M(x_i)}{M(x_j)}\times(x_i-x_j)i,j=1,2,\dots,n\text{ and }i\neq j\\
&C_{ij}^{(1)}=-\sum_{j=1,i\neq j}^{n}C_{ij}^{(1)}\;i=j
\end{aligned}
\tag{24}
$$

Table 1 The dimensionless natural frequency of the laminated nanopanel for different types of boundary conditions, numbers of grid points and patterns when a/b = 6.5, h = a/9, R_1 = R_2 = 10a and ΔT = 10 (K)

		N = M = 7	N = M = 9	N = M = 11	N = M = 13	N = M = 15
CFFF	N_t = [0 90 0]	0.0152839	0.0171311	0.0122786	0.0184308	0.0185104
	N_t = [0 90 0 90]	0.0320457	0.0333990	0.0379272	0.0340140	0.0340840
CSFS	N_t = [0 90 0]	0.0245107	0.0279184	0.0205209	0.0205209	0.0205209
	N_t = [0 90 0 90]	0.0411726	0.0410866	0.0407444	0.0407444	0.0407444
SSSS	N_t = [0 90 0]	0.0328041	0.0328039	0.0328039	0.0328039	0.0328039
	N_t = [0 90 0 90]	0.0685672	0.06850382	0.06844328	0.06839187	0.0683808
CSSS	N_t = [0 90 0]	0.0551124	0.05553747	0.05366811	0.05552384	0.0555205
	N_t = [0 90 0 90]	0.0971378	0.0989422	0.09917005	0.09929541	0.0992978
CCCC	N_t = [0 90 0]	0.0763170	0.0763555	0.0763567	0.0763567	0.0763567
	N_t = [0 90 0 90]	0.1388539	0.13889832	0.13889978	0.1389035	0.1389035

Table 2 The thermal buckling of the laminated nanopanel for various boundary conditions, numbers of grid points and length scale parameters when a/b = 6.5, h = a/10, R_1 = R_2 = 10a

		N = M = 7	N = M = 9	N = M = 11	N = M = 13	N = M = 15
CFFF	l/h = 0	1.449919	1.449102	1.449112	1.449111	1.449111
	l/h = 0.4	1.463493	1.462706	1.462714	1.462714	1.462714
CSFS	l/h = 0	2.466464	2.470683	2.470622	2.470649	2.470649
	l/h = 0.4	2.512817	2.514689	2.514825	2.514884	2.514884
SSSS	l/h = 0	4.292727	4.288484	4.288339	2.288339	2.288339
	l/h = 0.4	4.468242	4.431111	4.435274	4.434809	4.434809
CSSS	l/h = 0	1.449919	1.449102	1.449112	1.449111	1.449111
	l/h = 0.4	1.463493	1.462706	1.462714	1.462714	1.462714
CCCC	l/h = 0	2.466464	2.470683	2.470622	2.470649	2.470649
	l/h = 0.4	2.512817	2.514689	2.514825	2.514884	2.514884

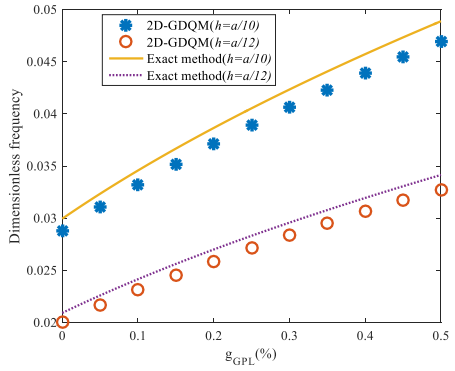

Fig. 2 The comparison of dimensionless frequency attained by analytical and 2D-GDQ procedures for laminated nanopanel

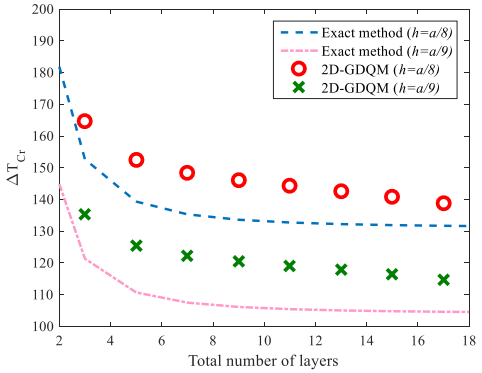

Fig. 3 The comparison of critical temperature attained by analytical and 2D-GDQ procedures for laminated nanopanel

where

$$M(x_i) = \prod_{j=1, j\neq i}^{n} (x_i - x_j) \tag{25}$$

Furthermore, the following relations represent the weighting coefficients of higher-order derivatives

$$\begin{aligned} &C_{ij}^{(r)} = r\left[C_{ij}^{(r-1)} \times C_{ij}^{(1)} - \frac{C_{ij}^{(r-1)}}{(x_i - x_j)}\right] \\ &i, j = 1,2,\ldots,n, \quad i \neq j \quad \text{and} \quad 2 \leq r \leq n-1 \\ &C_{ii}^{(r)} = -\sum_{j=1, i\neq j}^{n} C_{ij}^{(r)} \\ &i, j = 1,2,\ldots,n \quad \text{and} \quad 1 \leq r \leq n-1 \end{aligned} \tag{26}$$

In the current work, through x and y directions, a non-uniform set of points are presented as follows

$$\begin{aligned} x_i &= 0.5 \times a \times \left(1 - cos\left(\frac{(i-1)}{(N_i-1)}\right)\pi\right) i \\ &= 1,2,3,\dots,N_i \\ y_i &= 0.5 \times b \times \left(1 - cos\left(\frac{(j-1)}{(N_j-1)}\right)\pi\right) j \\ &= 1,2,3,\dots,N_j \end{aligned} \quad (27)$$

Freedom degrees are represented as

$$\begin{aligned} u(x,\theta,t) &= U(x,\theta) \times e^{i\omega t} \\ v(x,\theta,t) &= V(x,\theta) \times e^{i\omega t} \\ w(x,\theta,t) &= W(x,\theta) \times e^{i\omega t} \\ \psi_x(x,\theta,t) &= \Psi_x(x,\theta) \times e^{i\omega t} \\ \psi_\theta(x,\theta,t) &= \Psi_\theta(x,\theta) \times e^{i\omega t} \end{aligned} \quad (28)$$

Substitution of Eqs. (24) and (29) into governing equations, results in the following for natural frequency

$$\left\{\begin{bmatrix}[M_{dd}] & [M_{db}] \\ [M_{bd}] & [M_{bb}]\end{bmatrix}\omega^2 + \begin{bmatrix}[K_{dd}] & [K_{db}] \\ [K_{bd}] & [K_{bb}]\end{bmatrix}\right\}\begin{Bmatrix}\delta_d \\ \delta_b\end{Bmatrix} = 0 \quad (29)$$

where, boundary and domain points are defined by subscripts b and d, respectively. Additionally, the displacement vector is determined by the parameter of δ. The standard eigenvalue problem form of relation (30) is stated as follows

$$\begin{aligned} &[K^*]\{\delta_i\} = (\omega^2)[M^*]\{\delta_i\} \\ &[K^*] = [K_{dd} - K_{db}{K_{bb}}^{-1}K_{bd}] \\ &[M^*] = [M_{dd} - M_{db}{K_{bb}}^{-1}K_{bd}] \end{aligned} \quad (30)$$

4. Results

The numerical results of the critical temperature and frequency analysis of a doubly curved nanopanel are investigated based on the NSGT for the various boundary conditions. Sufficient number of grid points is necessary to achieve accurate results in GDQ method. It should be noted that in the current structure, clamped, simply, and free boundary conditions are presented as *C*, *S* and *F*, respectively. To achieve convergence results, different effective parameters of the system, such as boundary conditions and materials have been studied and compared. Besides, it could be observed that the system with four clamped edges has more stiffness than the system with (C-F-F-F) boundary condition. Also, by adding the number of layers, the dimensionless natural frequency enhances. On the basis of Table 1 the results are converged in 13 grid points. As Table 2 shows, the thermal buckling results are converged in the 15 grid points. Furthermore, it should be expressed that the changes in the non-dimensional length scale parameter have a direct influence on the thermal buckling load. It means an increment of the non-dimensional length scale leads to an increment trend in the thermal buckling load.

Table 3 Comparison of dimensionless frequency ($\omega h\sqrt{(2\rho(1+\upsilon)/E)}$) of an isotropic flat curved nanopanel (a = 10, E = 30e^6, υ = 0.3, ρ = 1, l = 0 and R_1= R_2 = ∞)

μ/h		a/h = 10		a/h = 20	
		b/a = 1	b/a = 2	b/a = 1	b/a = 2
0	Ref. (Żur *et al*. 2020)	0.0933	0.0590	0.0239	0.01500
	Present study	0.0927	0.0583	0.0234	0.01496
1	Ref. (Żur *et al*. 2020)	0.0852	0.0557	0.0218	-
	Present study	0.0849	0.0545	0.0213	0.01474

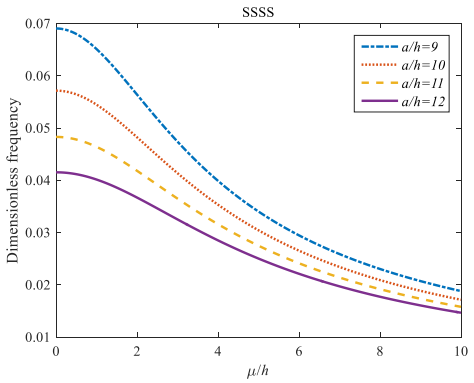

Fig. 4 The influences of a/h and μ/h on the non-dimensional frequency for the SSSS boundary conditions with l/h = 0.1 and $[0^0\ 90^0\ 0^0]$

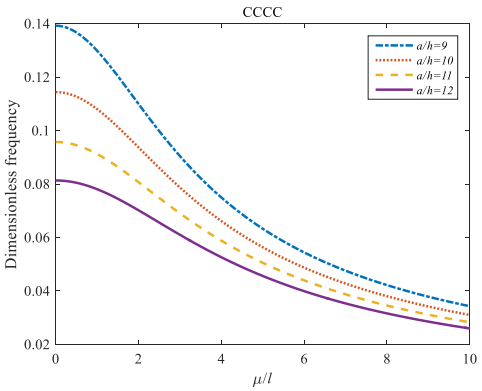

Fig. 5 The influences of a/h and μ/h on the non-dimensional frequency for the CCCC boundary conditions with l/h = 0.1 and $[0^0\ 90^0\ 0^0]$

4.1 Verification of numerical results

The validation has been performed by comparing the numerical results with analytical ones.

The obtained dimensionless frequency and the critical temperature of the laminated nanostructure with 2 exact and GDQ procedures are shown in Figs. 2 and 3, respectively, for various aspect ratios. An attractive result that obtained from Fig. 2 is that enhancement in the total number of

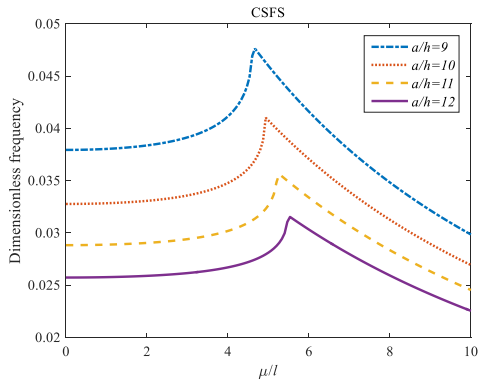

Fig. 6 The effects of a/h and μ/h on the non-dimensional frequency for the CSFS boundary conditions with l/h = 0.1 and $[0^0\ 90^0\ 0^0]$

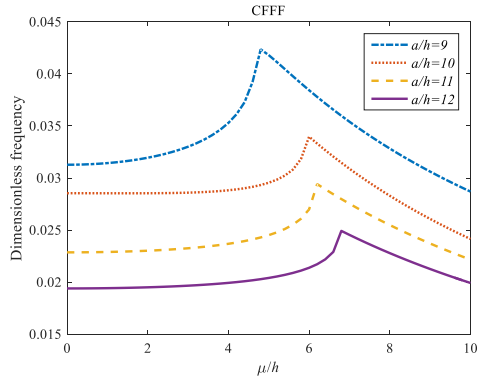

Fig. 7 The influences of a/h and μ/h on the non-dimensional frequency for the CFFF boundary conditions with l/h = 0.1 and $[0^0\ 90^0\ 0^0]$

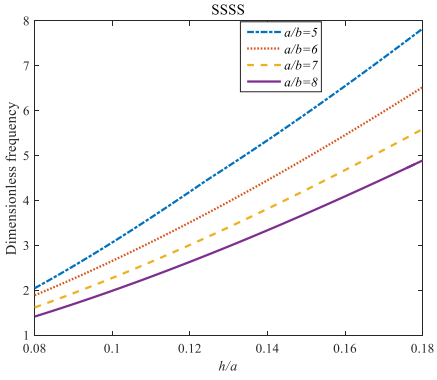

Fig. 8 The effects of R_1/a and a/b on the natural frequency for the SSSS boundary conditions (b/a = 6.5; h = a/10; N =11; R_1 = R_2 = 5b, μ/h = 0.1, l/h = 0.1 and $[90^0\ 0^0\ 90^0]$)

layers leads to lessening in the critical temperature. The reason for the discrepancy between the results is that, for analysis of a structure using the analytical method, we suggested a function according to the boundary conditions (Eq. (22)), but for analysis of a structure using the numerical method, we presented weighting coefficients and boundary, and domain nodes with the aid of boundary nodes

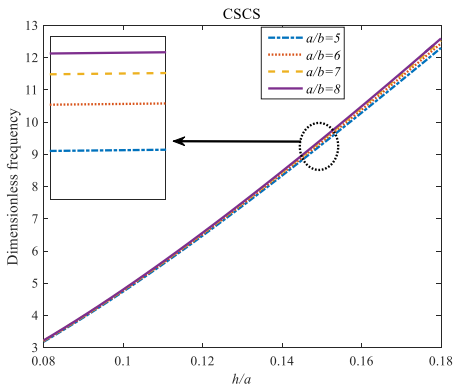

Fig. 9 The effects of R_1/a and a/b on the natural frequency for the CSCS boundary conditions (b/a = 6.5, h = a/10, N = 11, R_1 = R_2 = 5b, μ/h = 0.1, l/h = 0.1 and $[90^0\ 0^0\ 90^0]$)

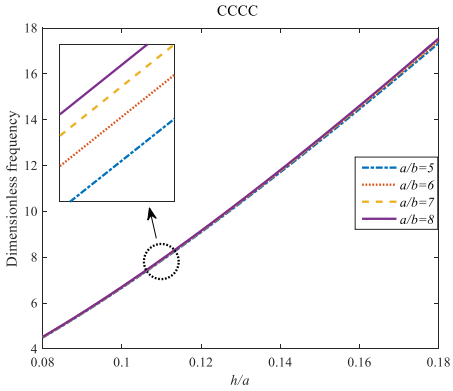

Fig. 10 The effects of h/a and a/b on the natural frequency for the CCCC boundary conditions (b/a = 6.5, h = a/10, N = 11, R_1 = R_2 = 5b, μ/h = 0.1, l/h = 0.1 and $[90^0\ 0^0\ 90^0]$)

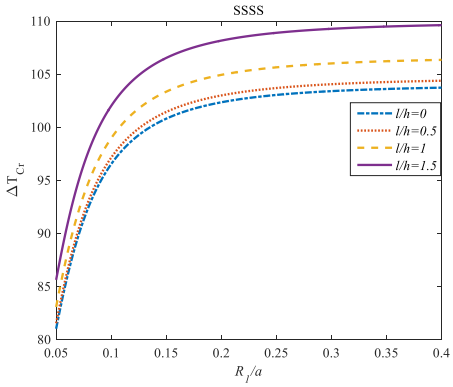

Fig. 11 The effects of l/h and R_1/a parameters on the thermal buckling of laminated nanopanel subjected to SSSS boundary conditions with μ/h = 0.1 and $[0^0\ 90^0\ 0^0\ 90^0\ 0^0]$)

for solving the problem (Eq. (30)).

For another verification for this work, according to Table 3, it is revealed that the proposed modeling can provide good agreement with Ref. (Żur *et al*. 2020).

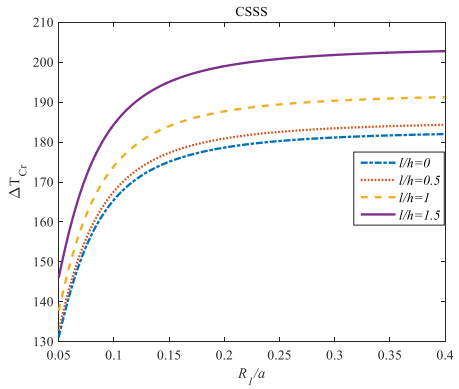

Fig. 12 The effects of l/h and R_1/a parameters on the thermal buckling of laminated nanopanel subjected to CSSS boundary conditions with μ/h = 0.1 and $[0^0\ 90^0\ 0^0\ 90^0\ 0^0]$)

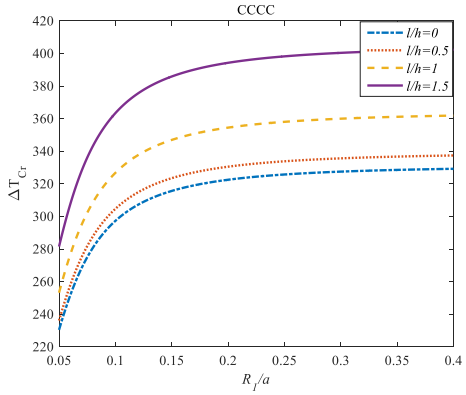

Fig. 13 The effects of l/h and R_1/a parameters on the thermal buckling of laminated nanopanel subjected to CCCC boundary conditions with μ/h = 0.1 and $[0^0\ 90^0\ 0^0\ 90^0\ 0^0]$)

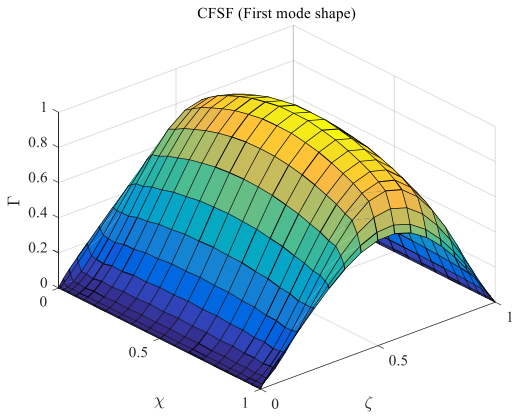

(a)

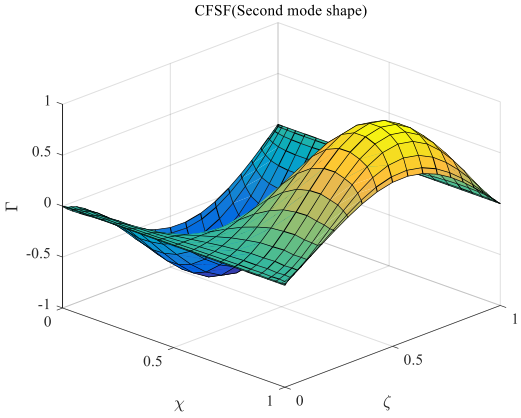

(b)

Fig. 14 The principal mode shapes of the laminated nanopanel under the CFSF boundary conditions with μ/h = 0.1 and l/h = 0.1 and $[0^0\ 90^0\ 0^0\ 90^0\ 0^0]$)

4.2 Parametric study

4.2.1 Influence of some parameters on the frequency of the laminated doubly curved nanopanel

Figs. 4, 5 and 6 face us with exposure about the influences of smaller aspect ratio (a/h) and nonlocal parameter to thickness ratio (μ/h) on the vibration response of the laminated nanopanel subjected to the SSSS, CCCC, CSFS and CFFF boundary conditions. This is because of the fact that an increase in a/h and μ/h) leads to a decrease in the stiffness of the structure, and causes natural frequency and stability to decrease.

According to Figs. 4 and 5, for CCCC and SSSS boundary conditions, by enhancing the μ/h parameter, the frequency response of the laminated nanopanel decreases exponentially. An impressive result that is coming up from Figs. 4 and 5 is that the impact of a/h parameter on the frequency of the system is dependent on the value of the nonlocal parameter. For better understanding, there is an indirect effect from a/h parameter on the dynamic response of the nano panel and this phenomenon is more intense at the higher value of the nonlocal parameter.

Figs. 6 and 7 present that for CSFS and CFFF boundary conditions and each value of the a/h parameter, firstly, an increment in the nonlocal parameter leads to an enhancement in the natural frequency of the structure as long as a maximum point appears, and then there can be seen an indirect relation between μ/h parameter and natural frequency of the nanostructure. For more detail, at the lower value of the μ/h parameter, there is a direct relation between this one and natural frequency, but at the higher value of the parameter, this relation changes from direct to indirect. In addition, for CSFS and CFFF boundary conditions, there is an indirect effect from a/h parameter on the dynamic response of the nano panel.

When one draws a comparison between Figs. 4, 5, 6 and 7, it can be inferred that while a boundary condition changes from free to simply and from simply to clamp natural frequencies increases. This results in an increase in the stability of the structure.

Figs. 8, 9 and 10 show natural frequency versus h/a parameter for different a/b parameters and boundary conditions. It can be seen from the graph that as the h/a parameter increases, the natural frequency increases, this leads to an increase in the stability of the structure.

By having remarkable attention to Figs. 8, 9 and 10 can apperceive, an attractive result is that laminated nanopanel is hardly dependent on the h/a parameter.

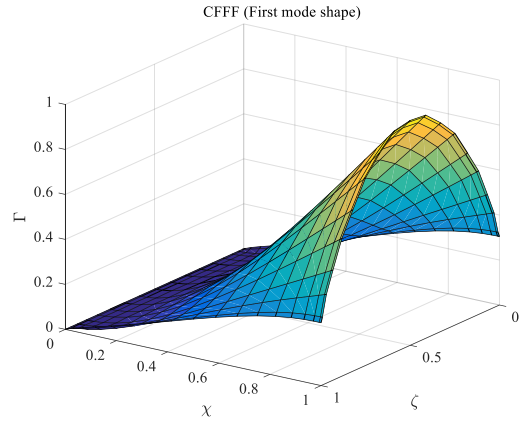

(a)

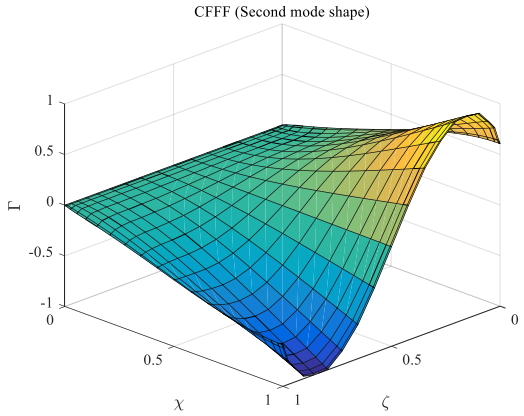

(b)

Fig. 15 The principal mode shapes of the laminated nanopanel under the CFSF boundary conditions with μ/h = 0.1 and l/h = 0.1 and $[0^0\ 90^0\ 0^0\ 90^0\ 0^0]$)

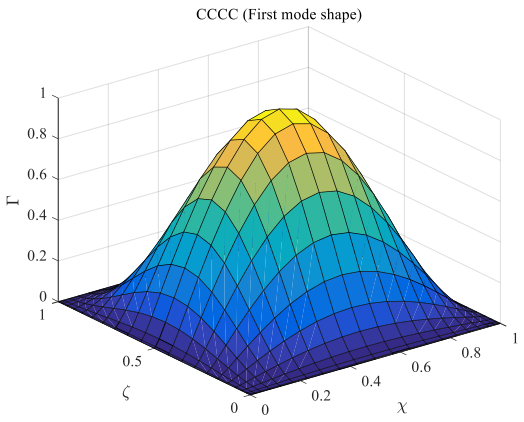

(a)

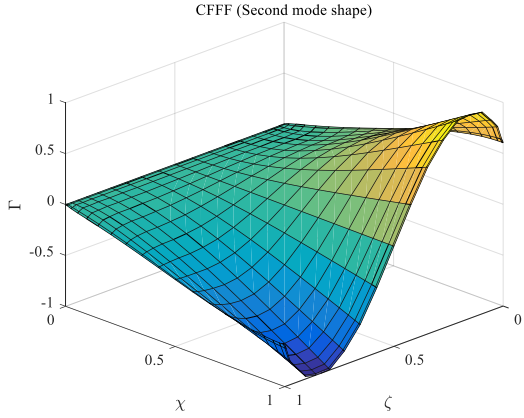

(b)

Fig. 16 The principal mode shapes of the laminated nanopanel under the CFSF boundary conditions with μ/h = 0.1 and l/h = 0.1 and $[0^0\ 90^0\ 0^0\ 90^0\ 0^0]$)

4.2.2 Influence of some parameters on the critical temperature of the laminated doubly curved nanopanels

Figs. 11, 12 and 13 indicate the influences of the length scale parameter (l/h) and dimensionless radius (R_1/a) of the nano panel, on the critical temperature of the nanostructure for various types of boundary conditions such as SSSS, CSSS and CCCC. As observed from Figs. 11,12 and 13, l/h and R_1/a parameters have direct influences on the critical temperature of the laminated nano panel. For better comprehension, an increment in the length scale and R_1/a parameters lead to an increase in the critical temperature of the laminated panel. Also, the influences of the length scale parameter on the thermal buckling load are under the effect of R_1/a parameter. As a detailed explanation, the influence of the l/h parameter on the thermal buckling load is more considerable at the higher value of R_1/a in comparison with the lower value of R_1/a. Additionally, at the higher value of the R_1/a parameter, the critical temperature does not have any significant change by increasing the R_1/a parameter.

When Figs. 11 to 13 are compared with each other, it can be inferred that while a boundary condition changes from simply to clamp critical temperature of the laminated nanopanel increases. This results in an increase in the stability of the structure.

In Figs. 14, 15, and 16, there are the two principal mode shapes of the nanopanel with CFSF, CCCC and CFFF boundary conditions. By comparing Figs. 14, 15 and 16 show that deformation of the laminated nanopanel under the CFFF boundary conditions is more distributed in comparison with the CCCC and CFSF boundary conditions.

5. Conclusions

In this study, frequency and thermal buckling analysis of the laminated nanopanel within the scope of NSGT and with the aid of 2D-GDQM were presented. By carrying out Hamilton's principle, the governing equations have been solved. The novelty of the current study was in considering the effects of laminated structure and thermal in addition of size effect on frequency, thermal buckling and dynamic deflections of the laminated nanopanel. By comparing the achieved results with those that existed in the available literature, the validation was examined. According to the results, different parameters such as the ratio of shell curvatures (R_1/R_2), geometric parameters, N_t and NSG parameters affect the static and dynamic features of the system.

- The results showed the dependency of the effects of

the a/b parameter on the natural frequency on the values of the a/h parameter.

• The results illustrated that the effects of the R_1/a parameter on the frequency response of the laminated nanopanel is really dependent on the values of the l/h parameter.

• As it is clear, the dynamic stability of the nano-system, unlike static stability, can be affected by the nonlocal parameter indirectly.

References

Arani, A.G., Pourjamshidian, M., Arefi, M. and Arani, M. (2019), "Application of nonlocal elasticity theory on the wave propagation of flexoelectric functionally graded (FG) timoshenko nano-beams considering surface effects and residual surface stress", *Smart Struct. Syst., Int. J.*, **23**(2), 141-153. https://doi.org/10.12989/sss.2019.23.2.141.

Arefi, M. (2020), "Smart analysis of doubly curved piezoelectric nano shells: Electrical and mechanical buckling analysis", *Smart Struct. Syst., Int. J.*, **25**(4), 471-486. https://doi.org/10.12989/sss.2020.25.4.471.

Arefi, M. and Rabczuk, T. (2019), "A nonlocal higher order shear deformation theory for electro-elastic analysis of a piezoelectric doubly curved nano shell", *Compos. Part B Eng.*, **168**, 496-510. https://doi.org/10.1016/j.compositesb.2019.03.065.

Arefi, M. and Civalek, O. (2020), "Static analysis of functionally graded composite shells on elastic foundations with nonlocal elasticity theory", *Arch. Civ. Mech. Eng.*, **20**(1), 1-17. https://doi.org/10.1007/s43452-020-00032-2.

Arefi, M. and Soltan Arani, A.H. (2020), "Nonlocal vibration analysis of the three-layered FG nanoplates subjected to applied electric potential considering thickness stretching effect", *Proc. Inst. Mech. Eng. L*, **2020**, 1464420720928378. https://doi.org/10.1177/1464420720928378.

Arefi, M., Bidgoli, E.M.R., Dimitri, R., Bacciocchi, M. and Tornabene, F. (2019a), "Nonlocal bending analysis of curved nanobeams reinforced by graphene nanoplatelets", *Compos. Part B Eng.*, **166**, 1-12. https://doi.org/10.1016/j.compositesb.2018.11.092.

Arefi, M., Kiani, M. and Rabczuk, T. (2019b), "Application of nonlocal strain gradient theory to size dependent bending analysis of a sandwich porous nanoplate integrated with piezomagnetic face-sheets", *Compos. Part B Eng.*, **168**, 320-333. https://doi.org/10.1016/j.compositesb.2019.02.057.

Arefi, M., Mohammad-Rezaei Bidgoli, E. and Civalek, O. (2020a), "Bending response of FG composite doubly curved nanoshells with thickness stretching via higher-order sinusoidal shear theory", *Mech. Based Des. Struct. Mach.*, **2020**, 1-29. https://doi.org/10.1080/15397734.2020.1777157.

Arefi, M., Zamani, M. and Kiani, M. (2020b), "Smart electrical and magnetic stability analysis of exponentially graded shear deformable three-layered nanoplate based on nonlocal piezo-magneto-elasticity theory", *J. Sandw. Struct. Mater.*, **22**(3), 599-625. https://doi.org/10.1177/1099636218760667.

Bagheri, H., Kiani, Y. and Eslami, M. (2019), "Asymmetric compressive stability of rotating annular plates", *Eur. J. Comput. Mech.*, **2019**, 1-21. https://doi.org/10.1080/17797179.2018.1560989.

Bai, B., Li, H., Zhang, W. and Cui, Y. (2020), "Application of extremum response surface method-based improved substructure component modal synthesis in mistuned turbine bladed disk", *J. Sound Vib.*, **472**, 115210. https://doi.org/10.1016/j.jsv.2020.115210.

Dai, T., Dai, H.L. and Lin, Z.Y. (2019), "Multi-field mechanical behavior of a rotating porous FGMEE circular disk with variable thickness under hygrothermal environment", *Compos. Struct.*, **210**, 641-656. https://doi.org/10.1016/j.compstruct.2018.11.077.

Dehshahri, K., Nejad, M.Z., Ziaee, S., Niknejad, A. and Hadi, A. (2020), "Free vibrations analysis of arbitrary three-dimensionally FGM nanoplates", *Adv. Nano Res., Int. J.*, **8**(2), 115-134. https://doi.org/10.12989/anr.2020.8.2.115.

Ebrahimi, F. and Jafari, A. (2017), "Investigating vibration behavior of smart imperfect functionally graded beam subjected to magnetic-electric fields based on refined shear deformation theory", *Adv. Nano Res., Int. J.*, **5**(4), 281-301. https://doi.org/10.12989/anr.2017.5.4.281.

Ebrahimi, F. and Salari, E. (2019), "Effect of non-uniform temperature distributions on nonlocal vibration and buckling of inhomogeneous size-dependent beams", *Adv. Nano Res., Int. J.*, **6**(4), 377-397. https://doi.org/10.12989/anr.2018.6.4.377.

Ebrahimi, F., Karimiasl, M. and Mahesh, V. (2019a), "Vibration analysis of magneto-flexo-electrically actuated porous rotary nanobeams considering thermal effects via nonlocal strain gradient elasticity theory", *Adv. Nano Res., Int. J.*, **7**(4), 223-231. https://doi.org/10.12989/anr.2019.7.4.223.

Ebrahimi, F., Karimiasl, M., Civalek, Ö. and Vinyas, M. (2019b), "Surface effects on scale-dependent vibration behavior of flexoelectric sandwich nanobeams", *Adv. Nano Res., Int. J.*, **7**(2), 77-88. https://doi.org/10.12989/anr.2019.7.2.077.

Ebrahimi, F., Jafari, A. and Selvamani, R. (2020), "Thermal buckling analysis of magneto-electro-elastic porous FG beam in thermal environment", *Adv. Nano Res., Int. J.*, **8**(1), 83-94. https://doi.org/10.12989/anr.2020.8.1.083.

Ehyaei, J. and Daman, M. (2017), "Free vibration analysis of double walled carbon nanotubes embedded in an elastic medium with initial imperfection", *Adv. Nano Res., Int. J.*, **5**(2), 179-192. https://doi.org/10.12989/anr.2017.5.2.179.

Emdadi, M., Mohammadimehr, M. and Navi, B.R. (2019), "Free vibration of an annular sandwich plate with CNTRC facesheets and FG porous cores using Ritz method", *Adv. Nano Res., Int. J.*, **7**(2), 109-123. https://doi.org/10.12989/anr.2019.7.2.109.

Ghannadpour, S. and Moradi, F. (2019), "Nonlocal nonlinear analysis of nano-graphene sheets under compression using semi-Galerkin technique", *Adv. Nano Res., Int. J.*, **7**(5), 311-324. https://doi.org/10.12989/anr.2019.7.5.311.

Gholami, R. and Ansari, R. (2019), "On the nonlinear vibrations of polymer nanocomposite rectangular plates reinforced by graphene nanoplatelets: a unified higher-order shear deformable model", *Iran. J. Sci. Technol. Trans. Mech. Eng.*, **43**(1), 603-620. https://doi.org/10.1007/s40997-018-0182-9.

Gunasekaran, V., Pitchaimani, J. and Chinnapandi, L.B.M. (2020), "Analytical investigation on free vibration frequencies of polymer nano composite plate: Effect of graphene grading and non-uniform edge loading", *Mater. Today Commun.*, **24**, 100910. https://doi.org/10.1016/j.mtcomm.2020.100910.

Hu, Y. and Wang, T. (2016), "Nonlinear free vibration of a rotating circular plate under the static load in magnetic field", *Nonlin. Dyn.*, **85**(3), 1825-1835. https://doi.org/10.1007/s11071-016-2798-x.

Hussain, M., Naeem, M.N., Tounsi, A. and Taj, M. (2019), "Nonlocal effect on the vibration of armchair and zigzag SWCNTs with bending rigidity", *Adv. Nano Res., Int. J.*, **7**(6), 431-442. https://doi.org/10.12989/anr.2019.7.6.431.

Javani, M., Kiani, Y. and Eslami, M. (2020), "Thermal buckling of FG graphene platelet reinforced composite annular sector plates", *Thin-Wall. Struct.*, **148**, 106589. https://doi.org/10.1016/j.tws.2019.106589.

Karami, B., Shahsavari, D., Janghorban, M. and Tounsi, A. (2019), "Resonance behavior of functionally graded polymer composite nanoplates reinforced with graphene nanoplatelets", *Int. J.*

Mech. Sci., **156**, 94-105. https://doi.org/10.1016/j.ijmecsci.2019.03.036.

Karimiasl, M., Ebrahimi, F. and Vinyas, M. (2019), "Nonlinear vibration analysis of multiscale doubly curved piezoelectric composite shell in hygrothermal environment", *J. Intell. Mater. Syst. Struct.*, **30**(10), 1594-1609. https://doi.org/10.1177/1045389X19835956.

Khosravi, F., Hosseini, S.A., Hamidi, B.A., Dimitri, R. and Tornabene, F. (2020), "Nonlocal torsional vibration of elliptical nanorods with different boundary conditions", *Vibration*, **3**(3), 189-203. https://doi.org/10.3390/vibration3030015.

Kumar, B.R. (2018), "Investigation on mechanical vibration of double-walled carbon nanotubes with inter-tube Van der waals forces", *Adv. Nano Res., Int. J.*, **6**(2), 135-145. https://doi.org/10.12989/anr.2018.6.2.135.

Liu, D., Li, Z., Kitipornchai, S. and Yang, J. (2019), "Three-dimensional free vibration and bending analyses of functionally graded graphene nanoplatelets-reinforced nanocomposite annular plates", *Compos. Struct.*, **229**, 111453. https://doi.org/10.1016/j.compstruct.2019.111453.

Mahinzare, M., Ranjbarpur, H. and Ghadiri, M. (2018), "Free vibration analysis of a rotary smart two directional functionally graded piezoelectric material in axial symmetry circular nanoplate", *Mech. Syst. Signal Process.*, **100**, 188-207. https://doi.org/10.1016/j.ymssp.2017.07.041.

Mahinzare, M., Alipour, M.J., Sadatsakkak, S.A. and Ghadiri, M. (2019), "A nonlocal strain gradient theory for dynamic modeling of a rotary thermo piezo electrically actuated nano FG circular plate", *Mech. Syst. Signal Process.*, **115**, 323-337. https://doi.org/10.1016/j.ymssp.2018.05.043.

Malikan, M., Nguyen, V.B. and Tornabene, F. (2018), "Damped forced vibration analysis of single-walled carbon nanotubes resting on viscoelastic foundation in thermal environment using nonlocal strain gradient theory", *Eng. Sci. Technol.*, **21**(4), 778-786. https://doi.org/10.1016/j.jestch.2018.06.001.

Mohammad-Rezaei Bidgoli, E. and Arefi, M. (2019), "Free vibration analysis of micro plate reinforced with functionally graded graphene nanoplatelets based on modified strain-gradient formulation", *J. Sandw. Struct Mater.*, 1099636219839302. https://doi.org/10.1177/1099636219839302.

Mohseni, A. and Shakouri, M. (2020), "Natural frequency, damping and forced responses of sandwich plates with viscoelastic core and graphene nanoplatelets reinforced face sheets", *J. Vib. Control*, 1077546319893453. https://doi.org/10.1177/1077546319893453.

Muc, A. (2011), "SHM of composite cylindrical multilayered shells with delaminations", *Proceedings of the IUTAM Symposium on Dynamics Modeling and Interaction Control in Virtual and Real Environments*, Budapest, Hungary, June. https://doi.org/10.1007/978-94-007-1643-8_25.

Muc, A. (2020), "Non-local approach to free vibrations and buckling problems for cylindrical nano-structures", *Compos. Struct.*, **250**, 112541. https://doi.org/10.1016/j.compstruct.2020.112541.

Muc, A. and Chwał, M. (2011), "Vibration control of defects in carbon nanotubes", *Proceedings of the IUTAM Symposium on Dynamics Modeling and Interaction Control in Virtual and Real* Environments, Budapest, Hungary, June. https://doi.org/10.1007/978-94-007-1643-8_27.

Muc, A. and Ulatowska, A. (2012), "Local fibre reinforcement of holes in composite multilayered plates", *Compos. Struct.*, **94**(4), 1413-1419. https://doi.org/10.1016/j.compstruct.2011.11.017.

Muc, A., Chwał, M. and Stawiarski, A. (2019), "Experimental and numerical analysis of heat convection in cylindrical composite structures with internal defects", *Adv. Compos. Lett.*, **28**, 0963693519879699. https://doi.org/10.1177/0963693519879699.

Natarajan, S., Chakraborty, S., Thangavel, M., Bordas, S. and Rabczuk, T. (2012), "Size-dependent free flexural vibration behavior of functionally graded nanoplates", *Comput. Mater. Sci.*, **65**, 74-80. https://doi.org/10.1016/j.commatsci.2012.06.031.

Nguyen-Thanh, N., Rabczuk, T., Nguyen-Xuan, H. and Bordas, S.P. (2010), "An alternative alpha finite element method (AαFEM) for free and forced structural vibration using triangular meshes", *J. Comput. Appl. Math.*, **233**(9), 2112-2135. https://doi.org/10.1016/j.cam.2009.08.117.

Nguyen-Thoi, T., Phung-Van, P., Rabczuk, T., Nguyen-Xuan, H. and Le-Van, C. (2013), "Free and forced vibration analysis using the n-sided polygonal cell-based smoothed finite element method (nCS-FEM)", *Int. J. Comput. Methods*, **10**(1), 1340008. https://doi.org/10.1142/S0219876213400082.

Nguyen-Thoi, T., Rabczuk, T., Lam-Phat, T., Ho-Huu, V. and Phung-Van, P. (2014), "Free vibration analysis of cracked Mindlin plate using an extended cell-based smoothed discrete shear gap method (XCS-DSG3)", *Theor. Appl. Fracture Mech.*, **72**, 150-163. https://doi.org/10.1016/j.tafmec.2014.02.004.

Nguyen-Thoi, T., Rabczuk, T., Ho-Huu, V., Le-Anh, L., Dang-Trung, H. and Vo-Duy, T. (2017), "An extended cell-based smoothed three-node Mindlin plate element (XCS-MIN3) for free vibration analysis of cracked FGM plates", *Int. J. Comput. Methods*, **14**(2), 1750011. https://doi.org/10.1142/S0219876217500116.

Noroozi, A.R., Malekzadeh, P., Dimitri, R. and Tornabene, F. (2020), "Meshfree radial point interpolation method for the vibration and buckling analysis of FG-GPLRC perforated plates under an in-plane loading", *Eng. Struct.*, **221**, 111000. https://doi.org/10.1016/j.engstruct.2020.111000.

Qin, Z., Yang, Z., Zu, J. and Chu, F. (2018), "Free vibration analysis of rotating cylindrical shells coupled with moderately thick annular plates", *Int. J. Mech. Sci.*, **142**, 127-139. https://doi.org/10.1016/j.ijmecsci.2018.04.044.

SafarPour, H., Hosseini, M. and Ghadiri, M. (2017), "Influence of three-parameter viscoelastic medium on vibration behavior of a cylindrical nonhomogeneous microshell in thermal environment: An exact solution", *J. Therm. Stress.*, **40**(11), 1353-1367. https://doi.org/10.1080/01495739.2017.1350827.

Sahmani, S., Aghdam, M.M. and Rabczuk, T. (2018), "Nonlocal strain gradient plate model for nonlinear large-amplitude vibrations of functionally graded porous micro/nano-plates reinforced with GPLs", *Compos. Struct.*, **198**, 51-62. https://doi.org/10.1016/j.compstruct.2018.05.031.

Salari, F.E.E. (2016), "Thermal loading effects on electro-mechanical vibration behavior of piezoelectrically actuated inhomogeneous size-dependent Timoshenko nanobeams", *Adv. Nano Res., Int. J.*, **4**(3), 197-228. https://doi.org/10.12989/anr.2016.4.3.197.

Shafiei, N., Mirjavadi, S.S., Afshari, B.M., Rabby, S. and Hamouda, A. (2017), "Nonlinear thermal buckling of axially functionally graded micro and nanobeams", *Compos. Struct.*, **168**, 428-439. https://doi.org/10.1016/j.compstruct.2017.02.048.

Shahsavari, D., Karami, B. and Janghorban, M. (2019), "Size-dependent vibration analysis of laminated composite plates", *Adv. Nano Res., Int. J.*, **7**(5), 337-349. https://doi.org/10.12989/anr.2019.7.5.337.

Sofiyev, A.H., Mammadov, Z., Dimitri, R. and Tornabene, F. (2020), "Vibration analysis of shear deformable carbon nanotubes-based functionally graded conical shells resting on elastic foundations", *Math. Methods Appl. Sci.*, In Press. https://doi.org/10.1002/mma.6674

Song, M., Li, X., Kitipornchai, S., Bi, Q. and Yang, J. (2019), "Low-velocity impact response of geometrically nonlinear functionally graded graphene platelet-reinforced nanocomposite plates", *Nonlin. Dyn.*, **95**(3), 2333-2352.

https://doi.org/10.1007/s11071-018-4695-y.
Thai, C.H., Ferreira, A., Tran, T. and Phung-Van, P. (2019), "Free vibration, buckling and bending analyses of multilayer functionally graded graphene nanoplatelets reinforced composite plates using the NURBS formulation", *Compos. Struct.*, **220**, 749-759. https://doi.org/10.1016/j.compstruct.2019.03.100.
Thai, C.H., Nguyen-Xuan, H., Nguyen-Thanh, N., Le, T.H., Nguyen-Thoi, T. and Rabczuk, T. (2012), "Static, free vibration, and buckling analysis of laminated composite Reissner-Mindlin plates using NURBS-based isogeometric approach", *Int. J. Num. Methods Eng.*, **91**(6), 571-603. https://doi.org/10.1002/nme.4282.
Tornabene, F. (2009), "Free vibration analysis of functionally graded conical, cylindrical shell and annular plate structures with a four-parameter power-law distribution", *Comput. Methods Appl. Mech. Eng.*, **198**(37-40), 2911-2935. https://doi.org/10.1016/j.cma.2009.04.011.
Tornabene, F. and Viola, E. (2009), "Free vibration analysis of functionally graded panels and shells of revolution", *Meccanica*, **44**(3), 255-281. https://doi.org/10.1007/s11012-008-9167-x.
Tornabene, F., Viola, E. and Inman, D.J. (2009), "2-D differential quadrature solution for vibration analysis of functionally graded conical, cylindrical shell and annular plate structures", *J. Sound Vib.*, **328**(3), 259-290. https://doi.org/10.1016/j.jsv.2009.07.031.
Tornabene, F., Viola, E. and Fantuzzi, N. (2013), "General higher-order equivalent single layer theory for free vibrations of doubly-curved laminated composite shells and panels", *Compos. Struct.*, **104**, 94-117. https://doi.org/10.1016/j.compstruct.2013.04.009.
Tornabene, F., Fantuzzi, N. and Bacciocchi, M. (2014), "Free vibrations of free-form doubly-curved shells made of functionally graded materials using higher-order equivalent single layer theories", *Compos. Part B Eng.*, **67**, 490-509. https://doi.org/10.1016/j.compositesb.2014.08.012.
Tornabene, F., Fantuzzi, N., Ubertini, F. and Viola, E. (2015a), "Strong formulation finite element method based on differential quadrature: A survey", *Appl. Mech. Rev.*, **67**(2), 020801. https://doi.org/10.1115/1.4028859.
Tornabene, F., Fantuzzi, N., Viola, E. and Batra, R.C. (2015b), "Stress and strain recovery for functionally graded free-form and doubly-curved sandwich shells using higher-order equivalent single layer theory", *Compos. Struct.*, **119**, 67-89. https://doi.org/10.1016/j.compstruct.2014.08.005.
Tornabene, F., Fantuzzi, N., Bacciocchi, M. and Viola, E. (2016), "Effect of agglomeration on the natural frequencies of functionally graded carbon nanotube-reinforced laminated composite doubly-curved shells", *Compos. Part B Eng.*, **89**, 187-218. https://doi.org/10.1016/j.compositesb.2015.11.016.
Tornabene, F., Fantuzzi, N. and Bacciocchi, M. (2017), "Linear static response of nanocomposite plates and shells reinforced by agglomerated carbon nanotubes", *Compos. Part B Eng.*, **115**, 449-476. https://doi.org/10.1016/j.compositesb.2016.07.011.
Tounsi, A., Benguediab, S., Semmah, A. and Zidour, M. (2013), "Nonlocal effects on thermal buckling properties of double-walled carbon nanotubes", *Adv. Nano Res., Int. J.*, **1**(1), 1-11. https://doi.org/10.12989/anr.2013.1.1.001.
Tran, T.T., Tran, V.K., Le, P.B., Phung, V.M., Do, V.T. and Nguyen, H.N. (2020), "Forced vibration analysis of laminated composite shells reinforced with graphene nanoplatelets using finite element method", *Adv. Civ. Eng.*, **2020**, 1471037. https://doi.org/10.1155/2020/1471037.
Valizadeh, N., Natarajan, S., Gonzalez-Estrada, O.A., Rabczuk, T., Bui, T.Q. and Bordas, S.P. (2013), "NURBS-based finite element analysis of functionally graded plates: Static bending, vibration, buckling and flutter", *Compos. Struct.*, **99**, 309-326. https://doi.org/10.1016/j.compstruct.2012.11.008.
Viola, E. and Tornabene, F. (2009), "Free vibrations of three parameter functionally graded parabolic panels of revolution", *Mech. Res. Commun.*, **36**(5), 587-594. https://doi.org/10.1016/j.mechrescom.2009.02.001.
Viola, E., Tornabene, F. and Fantuzzi, N. (2013), "Static analysis of completely doubly-curved laminated shells and panels using general higher-order shear deformation theories", *Compos. Struct.*, **101**, 59-93. https://doi.org/10.1016/j.compstruct.2013.01.002.
Wang, Y., Zeng, R. and Safarpour, M. (2020), "Vibration analysis of FG-GPLRC annular plate in a thermal environment", *Mech. Based Des. Struct. Mach.*, **2020**, 1-19. https://doi.org/10.1080/15397734.2020.1719508.
Wu, C.P., Chen, Y.H., Hong, Z.L. and Lin, C.H. (2018), "Nonlinear vibration analysis of an embedded multi-walled carbon nanotube", *Adv. Nano Res., Int. J.*, **6**(2), 163-182. https://doi.org/10.12989/anr.2018.6.2.163.
Wu, H., Zhu, J., Kitipornchai, S., Wang, Q., Ke, L.L. and Yang, J. (2020), "Large amplitude vibration of functionally graded graphene nanocomposite annular plates in thermal environments", *Compos. Struct.*, **239**, 112047. https://doi.org/10.1016/j.compstruct.2020.112047.
Yang, B., Kitipornchai, S., Yang, Y.F. and Yang, J. (2017), "3D thermo-mechanical bending solution of functionally graded graphene reinforced circular and annular plates", *Appl. Math. Model.*, **49**, 69-86. https://doi.org/10.1016/j.apm.2017.04.044.
Żur, K.K., Arefi, M., Kim, J. and Reddy, J. (2020), "Free vibration and buckling analyses of magneto-electro-elastic FGM nanoplates based on nonlocal modified higher-order sinusoidal shear deformation theory", *Compos. Part B Eng.*, **182**, 107601. https://doi.org/10.1016/j.compositesb.2019.107601.

CC